

Nanoscale

Accepted Manuscript



This is an *Accepted Manuscript*, which has been through the Royal Society of Chemistry peer review process and has been accepted for publication.

Accepted Manuscripts are published online shortly after acceptance, before technical editing, formatting and proof reading. Using this free service, authors can make their results available to the community, in citable form, before we publish the edited article. We will replace this *Accepted Manuscript* with the edited and formatted *Advance Article* as soon as it is available.

You can find more information about *Accepted Manuscripts* in the [Information for Authors](#).

Please note that technical editing may introduce minor changes to the text and/or graphics, which may alter content. The journal's standard [Terms & Conditions](#) and the [Ethical guidelines](#) still apply. In no event shall the Royal Society of Chemistry be held responsible for any errors or omissions in this *Accepted Manuscript* or any consequences arising from the use of any information it contains.



A Smart Core-sheath Nanofiber that Captures and Releases Red Blood Cells from the Blood

Q. Shi,^{*a} J. Hou,^a C. Zhao,^b Z. Xin,^{*b} J. Jin,^a C. Li,^a S.-C. Wong^c and J. Yin^a

Received 00th January 20xx,
Accepted 00th January 20xx

DOI: 10.1039/x0xx00000x

www.rsc.org/

A smart core-sheath nanofiber for non-adherent cell capture and release is demonstrated. The nanofibers are fabricated by single-spinneret electrospinning of poly (*N*-isopropylacrylamide) (PNIPAAm), polycaprolactone (PCL) and nattokinase (NK) solution blends. The self-assembly of PNIPAAm and PCL blends during the electrospinning generates the core-sheath PCL/PNIPAAm nanofibers with PNIPAAm as the sheath. The PNIPAAm-based core-sheath nanofibers are switchable between hydrophobicity to hydrophilicity with the temperature change and enhance the stability in the blood. When the nanofibers contact the blood, the NK is released from the nanofibers to resist platelet adhesion on the nanofiber surface, facilitating the direct capture and isolation of red blood cells (RBCs) from the blood above phase-transition temperature of PNIPAAm. Meanwhile, the captured RBCs are readily released from the nanofibers with the temperature stimuli in an undamaged manner. The release efficiency of up to 100% is obtained while maintaining cellular integrity and function. This work presents the promising nanofibers to effectively capture non-adherent cells and release for subsequent molecular analysis and diagnosis of single cells.

1. INTRODUCTION

Polymer nanofibers are finding an ever-increasing range of applications, including sensors, electronic devices, filter fabrics and medical/pharmaceutical application.^{1,2} Among the various nanofiber fabrication techniques, electrospinning has been investigated extensively due to its high throughput in a continuous process under mild conditions and its flexibility in controlling the fiber diameter from micrometer to nanometer scales.³⁻⁵ In addition, electrospinning is applicable to almost any soluble or fusible polymer and any substrate.^{6,7} Recently, because the extremely large surface area and porosity of nanofibers enhance the interactions between cells and nanofibers, various nanofibers have been fabricated towards the application in cell capture and release.⁸⁻¹⁰ However, electrospun nanofibers are usually ineffective in capturing and isolating non-adherent cells, such as major subgroups of blood cells, primary cells, or cell lines.^{11,12} In addition, the nanofibers typically fail to gently release captured cells in an undamaged

manner, which rises to significant challenges for subsequent molecular analysis and illness detection.¹³ Furthermore, the nanofibers often activate the platelets in the blood and induce platelet adhesion on the blood-contacting surface, resulting in low efficiency to isolate the targeted cells from the blood.¹⁴⁻¹⁶ Thus, it is highly desired to fabricate nanofibers for capturing non-adherent cells effectively from the blood and readily releasing the captured cells without injure.

A strategy to capture and release non-adherent cells is to utilize the smart nanofibers. The smart nanofibers are mainly fabricated from stimuli-responsive polymers.¹⁷ Nanoscale structures inherent to stimuli-responsive polymers render the nanofiber highly sensitive responses to external stimuli, and the incorporation of stimuli-responsive polymers into nanofibers enables a precision "on-off" switch to manipulate the morphology and function of the nanofibers.⁸ PNIPAAm-based nanofibers are typical thermo-responsive nanofibers with phase transition between hydrophilicity and hydrophobicity (~32°C), which are promise candidates for cell capture and release.¹⁸ PNIPAAm can be readily electrospun into the nanofibers with other high molecular weight (M_w) polymers to generate hydrophilic-hydrophobic switchable nanofibers¹⁹ and to enhance the nanofiber stability in contact with water.²⁰ It has been reported that the single-spinneret electrospinning of PNIPAAm/PCL blends in the solution results in core-sheath nanofibers with PNIPAAm as the sheath.¹⁹ Therefore, electrospinning of PNIPAAm-based nanofibers extends the nanoscale effects to the macroscale, which not only enables precise manipulation of the nanofiber properties

^a State Key Laboratory of Polymer Physics and Chemistry, Changchun Institute of Applied Chemistry, Chinese Academy of Sciences, Changchun 130022, P. R. China
E-mail: shiqiang@ciac.ac.cn, Tel: +86 431 85262161, Fax: +86 431 85262109

^b Department of Polymer, School of Chemistry and Chemical Engineering, Yantai University, Yantai, 264005, People's Republic of China
E-mail: xinzhirong2012@126.com

^c Department of Mechanical Engineering, University of Akron, Akron, Ohio 44325-3903, USA

[†] Electronic Supplementary Information (ESI) available: Electrospinning of polymer nanofibers; FTIR spectra and XPS spectra of PCL, PNIPAAm and PCL/PNIPAAm nanofibers; SEM images of PCL/PNIPAAm nanofibers with varied composition; PNIPAAm content on the sheath of nanofibers; Stability of core-sheath PCL/PNIPAAm nanofibers. See DOI: 10.1039/x0xx00000x

but also creates the opportunity for controllable cell capture and release.⁸

Anti-thrombus capability is necessary for the nanofibers to capture the non-adherent cells from the blood directly. Construction of hydrophilic surface, immobilization of bioactive reagents and loading with anti-thrombus agents are typical strategies to resist platelet adhesion on the nanofiber surface.^{21, 22} In view of simplicity and effectiveness, the nanofiber loaded with anti-thrombus agents is a good choice. Typical anti-thrombus agents include nattokinase (NK), heparin, lumbrokinase, streptokinase, urokinase, persantine and aspirin.²³ Among them, NK is of particular interest due to its effective biological thrombolysis of fibrin and thrombus in blood vessels, which is much stronger fibrinolytic activity than plasmin. NK is primarily isolated from a typical and popular soybean food in Japan “natto”.²⁴ The catalytic center of nattokinase is 275 amino acids with the molecular mass and isoelectric point of 27.7 kDa and 8.6.²⁵ Thus, the smart nanofibers loaded with NK can be fabricated with simple electrospinning. During contact the blood, the NK is expected to release from the nanofibers and interact with the blood to resist platelet adhesion.

Here, we fabricate PNIPAAm-based nanofibers loaded with NK to capture, isolate non-adherent cells from the blood and readily release the captured cells. Red blood cells (RBCs) are chosen as model cells because RBCs are typical non-adherent cells that take a key role in dilating blood vessels, oxygen delivery.^{26, 27} In addition, many early disease detection and treatment are performed depending on the RBCs analysis.^{28, 29} Our strategy is based on production of the thermo-responsive, core-sheath PCL/PNIPAAm/NK nanofibers with one-step electrospinning and resistance to platelet adhesion on the nanofiber during RBCs capture in the presence of NK. We demonstrate the self-assembly of PCL and PNIPAAm during electrospinning results in thermo-responsive core-sheath PNIPAAm/PCL/NK nanofibers; the release of NK from the nanofibers enables the nanofibers to resist platelet adhesion without obstruction of RBCs capture. The nanofibers are capable of capturing and isolating RBCs directly from the blood. Meanwhile, the hydrophilic-hydrophobic switch of nanofibers render the captured RBCs readily release from the nanofibers. The release efficiency of up to 100% is obtained while maintaining cellular integrity and function. Our work presents here not only generates a smart core-sheath nanofiber for RBCs capture and release, but also establishes the basic principle in designing blood-contacting biomaterials without damage to cells and activation of blood components.

2. EXPERIMENTAL SECTION

2.1. Materials.

Poly (*N*-isopropylacrylamide) (PNIPAAm), (M_n = 20000-40000, Aldrich), Polycaprolactone (PCL) (M_n = 70000-90000, Aldrich)

and bovine serum albumin (BSA) were purchased from Sigma-Aldrich. Nattokinase (NK, 410 IU/g) was obtained from Wako (Japan). Chloroform and dimethylformamide (DMF) were provided by Sigma-Aldrich. Phosphate buffered saline (PBS, 0.1 molL⁻¹, pH 7.4) solution was freshly prepared. Other chemicals were analytical grade and used without further purification. Milli-Q water (18.25 MΩcm) was used in all experiments.

2.2. Single-spinneret Electrospinning

The solution was prepared by dissolving PNIPAAm, PCL and NK in DMF/chloroform (2:3) at room temperature and stirring for 2 h. The ratio of PNIPAAm, PCL to NK was set as 5/5/1 and 5/5/2 with the total polymer concentration of 20 w/v%. Pure solutions of PNIPAAm (30 w/v%) and PCL (12 w/v %), and blending solution of PNIPAAm/PCL (10/10 w/w) were prepared for comparison (Fig. S1⁺, S2⁺). The polymer solutions were placed in a 1 mL syringe fitted with a metallic needle of 0.4 mm inner diameter. The syringe was fixed horizontally on the syringe pump (Model: OPON mini). And an electrode of high voltage power supply (Tianjin High-voltage Co.) was clamped to the metal needle tip. The flow rate of polymer solution was 0.7 mLh⁻¹, and the applied voltage was 18 kV. The tip-to-collector distance was set to 12 cm, and a grounded stationary rectangular metal collector (15 cm × 15 cm) covered by a piece of clean aluminum foil was used for the fiber collection.

2.3. Characterization

FTIR. The structure of electrospun nanofibers were analyzed by Bruker Fourier transition infrared (FTIR) spectrometer Vertex 70 equipped with an Attenuated Total Reflection (ATR) unit (ATR crystal 45 °) at a resolution of 4 cm⁻¹ for 32 scans.

SEM. The morphology of nanofiber was observed with field emission scanning electron microscopy (FESEM) by using a XL 30 ESEM FEG (FEI Company) instrument equipped with an EDX spectroscopy attachment.

XPS. The surface composition of electrospun fibers were analyzed via X-ray photoelectron spectroscopy (XPS) by using VG Scientific ESCA MK II Thermo Advantage V 3.20 analyzer with Al/K (hν = 1486.6 eV) anode mono-X-ray source. The take-off angle for photoelectron analyzer was fixed at 90°. All binding energy (BE) values were referenced to the C_{1s} hydrocarbon peak at 284.6 eV. The atomic concentrations of the elements were calculated by their corresponding peak areas.

Contact Angle Measurements. Surface wettability of nanofiber platform was evaluated by the sessile drop method with a pure water droplet (ca. 3 μL) using a contact angle goniometer (DSA, KRUSS GMBH, Germany). The temperature-controlled experiments were performed using a custom-made heating plate with a PID-controller (Panasonic). The average value of five measurements made at different surface locations on the same sample was adopted as the contact angle.

2.4. NK Release Measurement

The electrospun PCL/PNIPAAm/NK nanofibers were incubated in PBS solution at 37 °C and 25 °C, respectively. Then, 1 mL solution was collected at 10 min to 3 h and amount of the released NK was measured using high-performance liquid chromatography (Waters 600 HPLC, evaporative light scattering detector) with a standard calibration curve. The release profile was normalized to the amount of NK initially loaded in PCL/PNIPAAm nanofibers.

2.5. Purified Platelet Adhesion

Fresh blood from healthy white rabbits was extracted via venipuncture through a 19-gauge butterfly needle into a standard blood collection tube containing 3.8 wt% sodium citrate [9:1 (v/v) blood/anticoagulant] (The experiments were carried out in accordance with the guidelines issued by the Ethical Committee of the Chinese Academy of Sciences. The Committee approved the experiments and the informed consent was obtained for any experimentation with human subjects.). Then, the whole blood sample was centrifuged at 1000 rpm (or equivalent to approximately 91 g-force) for 15 min to separate platelet rich plasma (PRP) and the RBCs concentrates. The supernatant after centrifugation was PRP and the sediment was the RBC concentrates.

The nanofibers were immersed in PBS (pH 7.4) at 37 °C for 20 min to equilibrate the surfaces. Then PRP was deposited onto samples and allowed to adhere for 30 min at 37 °C and 25 °C, respectively. Then, the sample was rinsed away by PBS for several times and fixed with a fresh solution of 2.5 wt% glutaraldehyde in PBS at 37 °C for 2 h. All samples were freeze-dried and finally sputter coated by gold. Platelet adhesion was characterized by a field-emission SEM (SEM, Sirion-100, FEI, USA).

2.6. Purified RBCs Capture and Release

The nanofibers were placed into cell culture plates and sterilized with UV irradiation for 15 min at 37 °C. Then the RBC concentrates were washed three times with isotonic saline [0.9% (w/v) of aqueous NaCl solution, pH 7.4]. Subsequently, the RBC pellets were re-suspended in normal saline to obtain an RBC suspension at 20% (v/v) hematocrit. Afterward, 80 μL of RBC suspension was dropped on the nanofiber surface and incubated for 20 min under static conditions at 37 °C and 25 °C, respectively. To observe the capture and release of RBCs on the nanofibers, 80 μL RBC suspension was dropped on the nanofiber surface and incubated for 20 min under static conditions at 37 °C. Some samples were carefully rinsed with pre-warmed isotonic saline and fixed with 2.5 vol% glutaraldehyde for 1 h at 37 °C. The others were continued to incubate at 25 °C for another 20 min, followed by rinsing with isotonic saline and fixing with 2.5 vol% glutaraldehyde for 1 h at 25 °C. Then, all the samples were freeze-dried. The nanofibers with the captured RBCs and those after RBCs release were visualized by SEM, and the released RBCs were observed by confocal laser scanning microscope (CLSM, LSM700-Zeiss, Germany). CLSM was equipped with an InGaN semiconductor laser (405 nm), an Ar laser (488 nm), and a He-Ne laser (555 nm). All samples were visualized using the same acquisition settings and analyzed using Zen 2011 software (Carl Zeiss).

2.7. Capture and Release of RBCs from the Blood

The fresh blood from healthy white rabbits was diluted with PBS at the ratio of 1/50. The number of RBCs in the fresh blood was determined to be $1 \times 10^6 \mu\text{L}^{-1}$. The capture and release of RBCs from the blood was performed according to procedure described in purified RBC capture and release (2.7). The captured RBCs on the nanofibers and the surface after RBCs release were visualized by FESEM. The analysis involved counting of captured RBCs by using free software Image-J. The data from multiple separate experiments were analyzed and reported as the mean \pm the standard error (SE) of the mean. The capture efficiency was defined as the ratio of captured RBCs to the RBCs in the sample blood. And the release efficiency was defined as the ratio of released RBCs to the captured RBCs.

3. RESULTS AND DISCUSSION

The thermo-responsive and core-sheath PCL/PNIPAAm/nattokinase (NK) nanofibers are fabricated to capture and release non-adherent cells (Fig. 1). NK is mixed with PNIPAAm and PCL in the DMF/chloroform solution for single-spinneret electrospinning. Due to the self-assembly of PCL and PNIPAAm blends, core-sheath PCL/PNIPAAm nanofibers with PNIPAAm as the sheath are generated. The reversible phase transition of PNIPAAm renders the nanofibers thermo-responsive and PCL/PNIPAAm core-sheath structure enhances the stability of nanofibers in water. When the nanofibers contact the fresh blood, NK releases from the nanofibers and prevents platelet adhesion on the fiber surface, which facilitates the RBCs capture above the phase-transition temperature of PNIPAAm ($\sim 32^\circ\text{C}$).³⁰ When the temperature decreases below 32°C , the switch from hydrophobicity to hydrophilicity enables the captured RBCs to release from the nanofibers without damage.

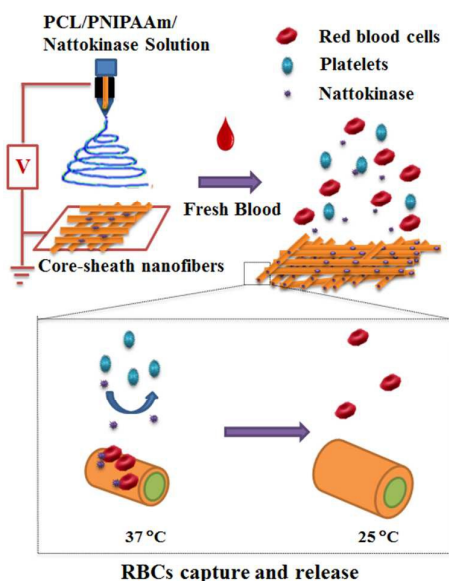


Fig. 1. Schematic procedure for fabrication of PCL/PNIPAAm core-sheath nanofibers containing nattokinase (NK) to capture and release red blood cells (RBCs) from the blood. The smart PCL/PNIPAAm/NK nanofibers are prepared with single-spinneret electrospinning. When nanofibers contact the fresh blood above phase-transition temperature of PNIPAAm ($\sim 32^\circ\text{C}$), the NK releases from the nanofibers to resist the platelet adhesion on the nanofiber surface, facilitating RBC capture on the nanofibers. The switch from hydrophobicity to hydrophilicity below 32°C enables RBCs to release from the nanofibers without damage.

3.1. Electrospinning of Core-sheath PCL/PNIPAAm Nanofibers

The PCL, PNIPAAm and NK are dissolved in the DMF/chloroform with the ratio of 5/5/1 and 5/5/2, respectively. The ratio of PCL to PNIPAAm (5/5) and total polymer weight of 20 wt% are chosen because the core-sheath structure of nanofibers is readily formed under these conditions (Fig.S3[†]). Fig. 2 shows the SEM images and TEM image of nanofibers with varied composition. The beads are observed on the PCL/PNIPAAm (5/5) nanofibers (Fig. 2a) because of the relatively low solution viscosity.³ The presence of NK tends to induce the bead formation on the nanofibers (Fig. 2b and 2c), which favors the NK encapsulation in the nanofibers.⁶ The TEM image of PCL/PNIPAAm/NK (5/5/2) nanofibers exhibits the obvious beaded feature of nanofibers (Fig. 2d). And the boundaries of the core-shell structure along the length of the fiber can be clearly seen (Fig. 2e). However, the dispersion of NK in the nanofibers can't be detected by the TEM, indicating NK is dispersed uniformly along the nanofiber or NK is mainly encapsulated in the beaded portions.

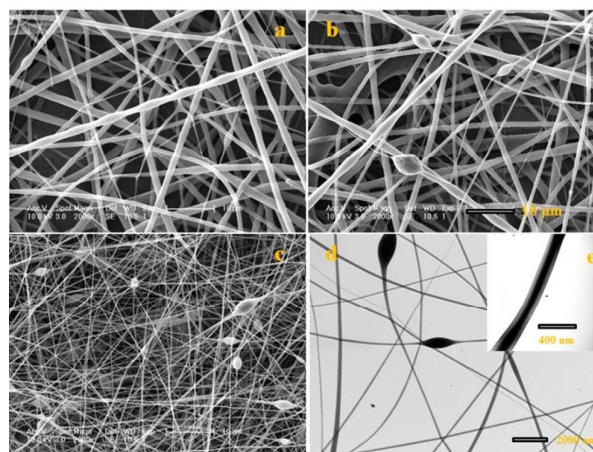


Fig. 2. SEM images and TEM image of nanofibers (a) PCL/PNIPAAm=5/5, (b) PCL/PNIPAAm/NK=5/5/1, (c) PCL/PNIPAAm/NK=5/5/2, (d) TEM image of PCL/PNIPAAm/NK nanofibers (5/5/2) and (e) core-sheath structure of the nanofiber.

The wide energy survey scan of nanofibers is shown in Fig. 3A. The binding energy (BE) at about 531 eV, 399 eV and 285 eV are attributed to O1s, N1s and C1s, respectively.³¹ Because XPS provides quantitative information of components in the outer layers of nanofibers, the wide energy survey scans is

used to calculate the surface coverage of PNIPAAm. According to the method provided by Chen et al., the surface coverage of PNIPAAm (% PNIPAAm) is estimated to be $6[N]/[C]$ from the wide energy survey scans.¹⁹ The composition of PNIPAAm and PCL on the nanofiber surface is exhibited in Fig. S4 and Tab. S1.

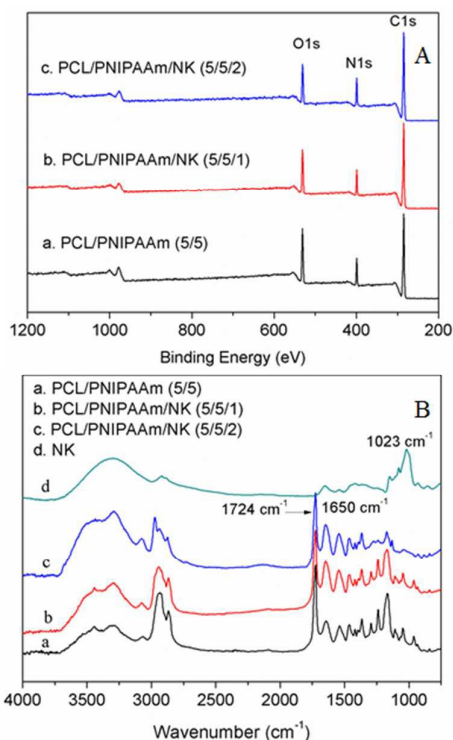


Fig. 3. XPS wide scan spectra and FTIR spectra of nanofibers. (a) PCL/PNIPAAm=5/5; (b) PCL/PNIPAAm/NK=5/5/1; (c) PCL/PNIPAAm/NK=5/5/2; (d) FTIR spectrum of NK.

The content of PNIPAAm on the surfaces is over 85% for the all nanofibers, demonstrating that the surfaces are enriched with PNIPAAm. The similar core-sheath PNIPAAm/PCL nanofibers have been obtained by Chen, et al.,¹⁹ and the formation of core-sheath structure is mainly attributed to the self-assembly of PCL/PNIPAAm blends during electrospinning.³² Because the phase separation of PNIPAAm and PCL is thermodynamically favored and the lower viscosity fluid (PNIPAAm) is kinetically located at the walls of the needle to attain a state of minimum energy dissipation,³³ a core-sheath structure is generated with PNIPAAm as the sheath and PCL as the core. Our result confirms that the presence of NK has no effect on the self-assembly of PNIPAAm/PCL blends during electrospinning. The core-sheath structure not only

renders the nanofibers thermo-responsive but also enhances the stability of nanofibers in water (Fig. S5⁺, Tab.S1⁺).

The FTIR spectra of nanofibers are shown in Fig. 3B. PCL/PNIPAAm nanofibers show a main peak at 1724 cm^{-1} and shoulder peak at 1650 cm^{-1} (Fig. S1⁺, Fig. 3B-a), which are assigned to carboxyl groups of PCL and PNIPAAm, respectively.³⁴ And NK exhibits the typical peak at 1023 cm^{-1} , attributing to the hydroxyl groups of NK (Fig. 3B-d). Because no signals from NK are detected on the FTIR spectra of PCL/PNIPAAm/NK nanofibers (Fig. 3B-b, c), it is confirmed that the NK is well encapsulated in the nanofibers. Thus, the loading amount of NK is assumed to be the same as the NK content in the polymer blends.²⁷

3.2. NK Release from PCL/PNIPAAm/NK Nanofibers

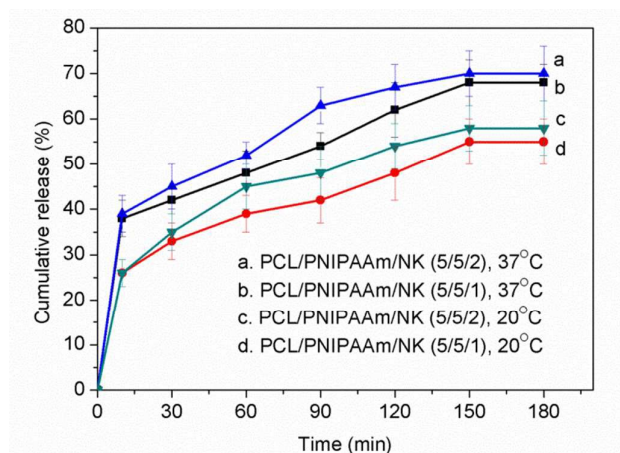


Fig. 4. Release profiles of NK from PCL/PNIPAAm/NK core-sheath nanofibers. NK release can last for 180 min both at $37\text{ }^{\circ}\text{C}$ and $20\text{ }^{\circ}\text{C}$, respectively. The release profile is normalized to the amount of NK initially loaded into PCL/PNIPAAm/NK nanofibers.

NK release profiles from PCL/PNIPAAm/PCL nanofibers in PBS solution are shown in Fig. 4. NK release is governed by the diffusion of drug through the matrix structure. The similar release profiles are observed at $25\text{ }^{\circ}\text{C}$ and $37\text{ }^{\circ}\text{C}$, but the cumulative release of NK is higher at $37\text{ }^{\circ}\text{C}$ (curve a Vs c). The higher loading content of NK in the nanofibers results in higher release rate (curve a Vs b). Both the releases can last more than 180 min, which are important for capture and release RBCs from the blood repeatedly. NK is one of thrombolytic enzymes, which not only possesses activity of plasminogen activator, but directly digests fibrin through limited

proteolysis.²³ Based on its food origin and relatively strong fibrinolytic activity, NK has gained the advantages over other commercially used agents in preventative and prolonged effects. Its fibrinolytic activity can be retained in the blood for more than 3 h.³⁵ Thus, the released NK is expected to resist the platelet activation and adhesion on the nanofiber surface by digesting the fibrin formed in the blood.

3.3. Thermo-responsive Nanofibers and Purified Platelets

Adhesion

Water contact angle (WCA) measurements are performed to confirm thermo-responsiveness of core-sheath nanofibers. As shown in the insets of Fig. 5, all the nanofibers are hydrophobic at 37°C. And the wettability of the nanofibers displays evident changes from hydrophobicity (WCA>120°) at 37°C to hydrophilicity (WCA < 24°) at 25°C. Furthermore, the nanofibers tend to be hydrophilic with increasing NK content in the nanofibers. For example, the PCL/PNIPAAm/NK (5/5/2) nanofiber is super-hydrophilic at 25°C with the WCA of 10°. Because PNIPAAm enriches on the nanofiber surface, the nanofiber switch is mainly caused by the phase transition of PNIPAAm sheath. At 25°C, the intermolecular hydrogen bonding between the PNIPAAm chains and water molecules is dominant, which renders nanofibers hydrophilic and PNIPAAm chains relaxed. Upon heating, the predominantly intermolecular hydrogen bonding is replaced by intramolecular hydrogen bonding between C=O and N-H groups along the PNIPAAm chains, resulting in hydrophobicity of nanofibers and collapsed PNIPAAm chains.¹⁹ The phase transition of PNIPAAm chains endows the PCL/PNIPAAm/NK nanofibers with the reversible hydrophobic-hydrophilic transition under the alternation of temperature (Fig.S6). The wettability of nanofiber affects the plasma protein adsorption on the webs. Bovine serum albumin (BSA) is used as a model protein to evaluate the protein adsorption on nanofibers at different temperatures. The results for BSA adsorption are listed in Tab. S2 (Supporting Information). Tab. S2 shows that the amount of protein adsorbed on the PNIPAAm-based nanofibers at 37°C is nearly four-fold increase compared with that adsorbed on the nanofibers at 25°C, and the presence of NK has slight effect on protein adsorption. The switch from the hydrophobicity to

hydrophilicity of nanofibers paves a facile way for cell capture and on-demand release.

To confirm the platelet-resistance of nanofibers, the purified platelet adhesion on the nanofibers is performed at 25 and 37°C, respectively. Platelets are highly adhesive in nature, and they are inclined to adhere on the hydrophobic surface but inert to the hydrophilic surface.¹⁶ Because of the hydrophobic surface of PCL/PNIPAAm nanofibers at 37°C, the platelet adheres on the nanofiber surface (Fig. 5a). In contrast, the PCL/PNIPAAm/NK nanofibers resist platelet adhesion at 37°C. Because no platelet adhesion on the PCL/PNIPAAm nanofibers is observed after the nanofibers are cultured with PRP in the presence of free NK at 37°C for 30 min (Fig. S7), it is reasonable that the NK released from the nanofibers endows the nanofibers with anti-thrombus ability²³ (Fig. 5b and 5c). All the nanofibers resist the platelet adhesion at 25°C because of the hydrophilicity of nanofibers (Fig. 5d-e). The resistance of nanofiber to platelet adhesion facilitates the RBCs capture directly from the blood.

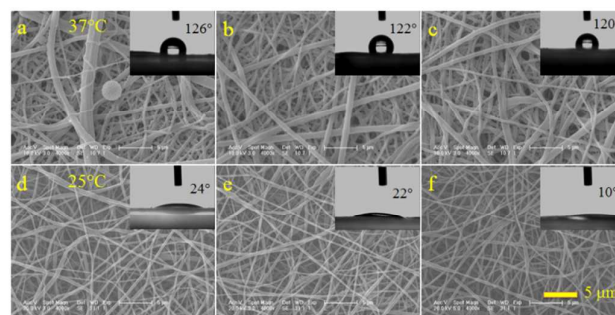


Fig. 5. Purified platelet adhesion on the nanofibers and water contact angle of nanofibers. (a), (d) PCL/PNIPAAm nanofibers; (b), (e) PCL/PNIPAAm/NK (5/5/1) nanofibers; (c), (f) PCL/PNIPAAm/NK (5/5/2) nanofibers. The corresponding WCA are provided as insets in each Figure. The nanofiber webs are hydrophobic (WCA>120°) at 37°C and hydrophilic (WCA<24°) at 25°C. The PCL/PNIPAAm/NK nanofibers show the platelet resistance both at 37°C and 25°C.

3.4. Purified RBCs Capture and Release

Purified RBCs capture and release mainly depends on the thermo-responsiveness of PCL/PNIPAA/NK core-sheath nanofibers. Purified RBCs capture is performed on the nanofiber webs at 37 °C. Due to the hydrophobic interactions between nanofibers with RBCs, purified RBCs are captured on the nanofiber webs. The number of captured RBCs on the

PCL/PNIPAAm is slightly higher than that on the PCL/PNIPAAm/NK nanofibers, indicating the presence of NK has little effects on the RBCs adhesion. After RBCs capture on the nanofibers, the nanofibers are transferred to a sterile cupboard at 25°C for 20 min, followed by PBS rinsing for several times. Most adhered RBCs release from the nanofibers (Fig. 6d-f) and CLSM images show that the released RBCs maintain the morphology of normal biconcave discs (insets of Fig. 6), demonstrating the captured RBCs maintain their normal function.²⁷

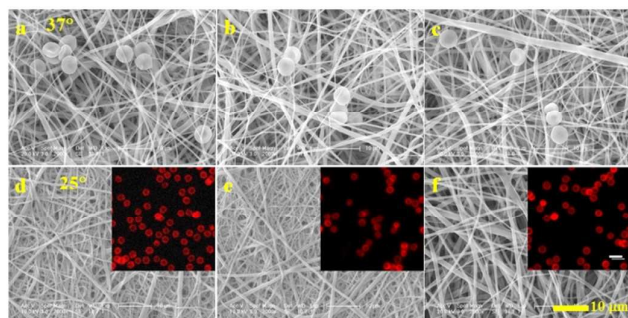


Fig. 6. SEM images of RBC capture and release on the nanofibers and CLSM images of released RBCs. (a), (d) RBC capture and release on PCL/PNIPAAm nanofibers; (b), (e) RBC capture and release on PCL/PNIPAAm/NK (5/5/1) nanofibers; (c), (f) RBC capture and release on PCL/PNIPAAm/NK (5/5/2) nanofibers; insets of (d), (e) and (f) are CLSM images of released RBCs from PCL/PNIPAAm, PCL/PNIPAAm/NK (5/5/1) and PCL/PNIPAAm/NK (5/5/2) nanofibers, respectively.

Our results confirm the switch between hydrophobicity and hydrophilicity of nanofibers enables the RBCs capture and release without damage. The current techniques for cell capture with bioactive ligand or antibodies often fail to gently release the captured cells.¹³ On the contrary, we employ the topographic structure of nanofibers and hydrophobic interactions to capture and release RBCs in an undamaged manner. The similar strategy has been utilized by Wang et al., who capture and release cancer cells based on hydrophobic interaction and topographic interaction.³⁶ Contrast to the monovalent adhesion, hydrophobic interaction enables the captured RBCs to release without injure to RBCs, facilitating the subsequent cell culture and single cell analysis.

3.5. Capture RBCs from the Blood and subsequent Release

The nanofibers that resist platelet adhesion but can adhere RBCs at 37°C find their application in capturing the RBCs from fresh blood. The diluted fresh blood with the RBCs concentration of $10^4 \mu\text{L}^{-1}$ is used to check the capture and release efficiency on the nanofibers. The RBCs capture efficiency and release efficiency exhibit the opposite tendencies with the increasing NK loading in the nanofibers (Fig. 7). The capture efficiency decreases in the order of PCL/PNIPAAm (5/5), PCL/PNIPAAm/NK (5/5/1) and PCL/PNIPAAm/NK (5/5/2). In contrast, the release efficiency increases in the order of PCL/PNIPAAm (5/5), PCL/PNIPAAm/NK (5/5/1) and PCL/PNIPAAm/NK (5/5/2). And the release efficiency approaches nearly 100% on PCL/PNIPAAm/NK (5/5/2) nanofibers. The opposite tendencies can be explained as follows: blood platelets adhere readily on the hydrophobic surfaces of nanofiber and release a number of biologically active substances upon activation such as α -granules to induce RBCs adhesion on the nanofibers.^{16, 37} For the PCL/PNIPAAm nanofibers, the platelet can adhere on the hydrophobic surface of nanofibers to induce subsequent RBCs adhesion, resulting in the highest capture efficiency of PCL/PNIPAAm nanofibers. However, platelets-RBCs interaction often reduces the deformability of RBCs and increases the adhesion of RBCs on the nanofibers,³⁸ which prevents the RBCs release from the nanofibers. As the consequence, the release efficiency of PCL/PNIPAAm nanofibers is lowest. The situation is completely changed for PCL/PNIPAAm/NK (5/5/2) nanofibers. Because the presence of NK resists the platelet adhesion on the nanofibers substantially,²³ the platelets have no effects on the RBCs adhesion. The number of captured RBCs is reduced, but the adhered RBCs maintain their biconcave shape and normal function. Therefore, the capture efficiency on PCL/PNIPAAm/NK (5/5/2) nanofibers is lowest but the release efficiency is highest. The above explanation is supported by Fig. 7a and 7b. Fig. 7a clearly shows that platelets induce RBCs to adhesion on the PCL/PNIPAAm nanofibers, but RBCs are deformed into the echinocytes with protrusions and spheroechinocytes. Fig. 7b exhibits the adhered RBCs on the PCL/PNIPAAm/NK (5/5/2) nanofibers with the typical biconcave shape. The ratio of RBC normal shape on these nanofibers further confirms our explanation. The ratio of

normal shape of captured RBCs appears the similar tendency as the release efficiency, which increases in the order of PCL/PNIPAAm (5/5), PCL/PNIPAAm/NK (5/5/1) and PCL/PNIPAAm/NK (5/5/2). Our work demonstrates that PCL/PNIPAAm/NK nanofibers capture the RBCs from the fresh blood successfully and effectively release the captured RBCs without damage to the cells.

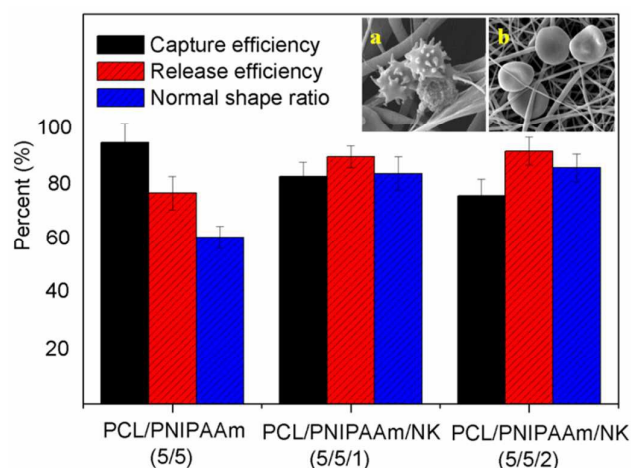


Fig. 7. Capture, release efficiencies of RBCs and the ratio of normal shape of captured RBCs on the nanofibers. (a) SEM image of captured platelets and RBCs on PCL/PNIPAAm (5/5) nanofibers, (b) SEM images of captured RBCs on PCL/PNIPAAm/NK (5/5/2) nanofibers.

Therefore, the smart core-sheath PCL/PNIPAAm/NK nanofibers gain the advantage on real-time, point-of-care cell detection and the subsequent molecular analysis.³⁹ In addition, as PNIPAAm can be substituted with other smart polymers,⁴⁰ and the designed cell-capture agents can be introduced to the nanofibers,⁴¹ the method presented here is universal to capture varied cells in the blood or body fluids. The nanofibers with simple fabrication and effective capture and release may potentially apply in molecular analysis and clinical diagnostics, particularly in cases when the relevant cells are derived from the blood of the patient.

4. CONCLUSIONS

In summary, the smart core-sheath nanofibers were developed to capture, isolate non-adherent cells from the blood and readily release captured cells. Our strategy was based on production of the thermo-responsive, core-sheath

PCL/PNIPAAm/NK nanofibers with one-step electrospinning and resistance to platelet adhesion on the nanofiber during RBCs capture with the aid of NK. We demonstrated that the self-assembly of PCL and PNIPAAm during electrospinning resulted in thermo-responsive core-sheath PCL/PNIPAAm/NK nanofibers; the release of NK from the nanofibers enabled the nanofibers to resist platelet adhesion; the nanofibers were capable of capturing and isolating RBCs directly from the blood. Meanwhile, the hydrophilic-hydrophobic switch of nanofibers rendered the captured RBCs readily release from the nanofibers; the release efficiency of nearly 100% was obtained while maintaining cellular integrity and function. Our work presented here not only fabricated a smart core-sheath nanofiber for RBCs capture and release, but also established the basic principle in non-adherent cells capture and release from the blood or biological fluid.

Acknowledgements

This work was supported by the financial support of the National Natural Science Foundation of China (Projects No. 51273199, 51573186 and 21274150).

Notes and references

- S. Hou, L. Zhao, Q. Shen, J. Yu, C. Ng, X. Kong, D. Wu, M. Song, X. Shi and X. Xu, *Angew. Chem. Int. Ed.*, 2013, 52, 3379-3383.
- L. Zhao, Y. T. Lu, F. Li, K. Wu, S. Hou, J. Yu, Q. Shen, D. Wu, M. Song and W. H. OuYang, *Adv. Mater.*, 2013, 25, 2897-2902.
- S. Agarwal, A. Greiner and J. H. Wendorff, *Prog. Polym. Sci.*, 2013, 38, 963-991.
- Q. Shi, S.-C. Wong, W. Ye, J. Hou, J. Zhao and J. Yin, *Langmuir*, 2012, 28, 4663-4671.
- Q. Shi, Q. Fan, X. Xu, W. Ye, J. Hou, S.-C. Wong and J. Yin, *Langmuir*, 2014, 30, 13549-13555.
- B. Sun, Y. Z. Long, H. D. Zhang, M. M. Li, J. L. Duvail, X. Y. Jiang and H. L. Yin, *Prog. Polym. Sci.*, 2014, 39, 862-890.
- X. Wang, B. Ding, J. Yu, and M. Wang, *Nano Today*, 2011, 6, 510-530.
- Y. J. Kim, M. Ebara and T. Aoyagi, *Angew. Chem.*, 2012, 124, 10689-10693.
- Q. Shen, L. Xu, L. Zhao, D. Wu, Y. Fan, Y. Zhou, W. H. OuYang, X. Xu, Z. Zhang and M. Song, *Adv. Mater.*, 2013, 25, 2368-2373.
- N. Zhang, Y. Deng, Q. Tai, B. Cheng, L. Zhao, Q. Shen, R. He, L. Hong, W. Liu, S. Guo, K. Liu, H. Tseng, B. Xiong and X. Z. Zhao, *Adv. Mater.*, 2012, 24, 2756-2760.
- M. Deutsch, A. Deutsch, O. Shirihai, I. Hurevich, E. Afrimzon, Y. Shafran and N. Zurgil, *Lab Chip*, 2006, 6, 995-1000.
- Y. Roupioz, N. Berthet - Duroure, T. Leïchl e, J. B. Pourciel, P. Mailley, S. Cortes, M.-B. Villiers, P.-N. Marceh, T. Livache and L. Nicu, *Small*, 2009, 5, 1493-1497.
- W. Zhao, C. H. Cui, S. Bose, D. Guo, C. Shen, W. P. Wong, K. Halvorsen, O. C. Farokhzad, G. S. L. Teo, J. A. Phillips, D. M.

- Dorfman, R. Karnike and J. M. Karp, *Proc. Natl. Acad. Sci. USA*, 2012, **109**, 19626-19631.
- 14 T. Ekblad, L. Faxälv, O. Andersson, N. Wallmark, A. Larsson, T. L. Lindahl and B. Liedberg, *Adv. Funct. Mater.*, 2010, **20**, 2396-2403.
- 15 S. T. Gunawan, K. Kempe, T. Bonnard, J. Cui, K. Alt, L. S. Law, X. Wang, E. Westein, G. K. Such, K. Peter, C.E. Hagemeyer and F. Caruso, *Adv. Mater.*, 2015, **27**, 5153-5157.
- 16 W. Ye, Q. Shi, S.-C. Wong, J. Hou, X. Xu and J. Yin, *Biomater. Sci.*, 2014, **2**, 1186-1194.
- 17 F. Yao, L. Xu, B. Lin and G.-D. Fu, *Nanoscale*, 2010, **2**, 1348-1357.
- 18 S. R. Deka, A. Quarta, R. Di Corato, A. Riedinger, R. Cingolani and T. Pellegrino, *Nanoscale*, 2011, **3**, 619-629.
- 19 M. Chen, M. Dong, R. Havelund, V. R. Regina, R. L. Meyer, F. Besenbacher and P. Kingshott, *Chem. Mater.*, 2010, **22**, 4214-4221.
- 20 L. Maggi, R. Bruni and U. Conte, *Inter. J. Pharm.*, 2000, **195**, 229-238.
- 21 C. K. Hashi, Y. Zhu, G.-Y. Yang, W. L. Young, B. S. Hsiao, K. Wang, B. Chu and S. Li, *Proc. Natl. Acad. Sci. USA*, 2007, **104**, 11915-11920.
- 22 B. W. Tillman, S. K. Yazdani, S. J. Lee, R. L. Geary, A. Atala and J. J. Yoo, *Biomaterials*, 2009, **30**, 583-588.
- 23 C. Chen, H. Duan, C. Gao, M. Liu, X. A. Wu, Y. Wei, X. Zhang and Z. Liu, *RSC Adv.*, 2014, **4**, 27422-27429.
- 24 H. Sumi, H. Hamada, H. Tsushima, H. Mihara and H. Muraki, *Experientia*, 1987, **43**, 1110-1111.
- 25 J.-G. Liu, J.-M. Xing, R. Shen, C.-L. Yang and H.-Z. Liu, *Biochem. Eng. J.*, 2004, **21**, 273-278.
- 26 J. R. Pawloski, D. T. Hess and J. S. Stamler, *Proc. Natl. Acad. Sci. USA*, 2005, **102**, 2531-2536.
- 27 Q. Shi, Q. Fan, W. Ye, J. Hou, S.-C. Wong, X. Xu and J. Yin, *ACS Appl. Mater. Interfaces*, 2014, **6**, 9808-9814.
- 28 R. Medzhitov, D. S. Schneider and M. P. Soares, *Science*, 2012, **335**, 936-941.
- 29 D. J. Schaer, P. W. Buehler, A. I. Alayash, J. D. Belcher and G. M. Vercellotti, *Blood*, 2013, **121**, 1276-1284.
- 30 H. G. Schild, *Prog. Polym. Sci.*, 1992, **17**, 163-249.
- 31 F. Xu, J. Li, S. Yuan, Z. Zhang, E. Kang and K. Neoh, *Biomacromolecules*, 2007, **9**, 331-339.
- 32 M. Wei, B. Kang, C. Sung and J. Mead, *Macro. Mater. Eng.*, 2006, **291**, 1307-1314.
- 33 X. Y. Sun, R. Shankar, H. G. Börner, T. K. Ghosh and R. J. Spontak, *Adv. Mater.*, 2007, **19**, 87-91.
- 34 T. Wu, Y. Zhang, X. Wang and S. Liu, *Chem. Mater.*, 2007, **20**, 101-109.
- 35 J. Kim, J.-H. Kim, K.-H. Choi, J. H. Kim, Y.-S. Song and J. Cha, *J. Agric. Food Chem.*, 2011, **59**, 8675-8682.
- 36 H. Liu, X. Liu, J. Meng, P. Zhang, G. Yang, B. Su, K. Sun, L. Chen, D. Han, S. Wang and L. Jiang, *Adv. Mater.*, 2013, **25**, 922-927.
- 37 H. A. Brittain, J. R. Eckman, R. A. Swerlick, R. J. Howard and T. M. Wick, *Blood*, 1993, **81**, 2137-2143.
- 38 J. Vallés, M. T. Santos, J. Aznar, M. Martínez, A. Moscardó, M. Piñón, M. J. Broekman and A. J. Marcus, *Blood*, 2002, **99**, 3978-3984.
- 39 J. Sun, Y. X. Yu and X.Y. Jiang, *Chem. Soc. Rev.*, 2014, **43**, 6239-6253.
- 40 M. R. Molla, P. Rangadurai, G. M. Pavan and S. Thayumanavan, *Nanoscale*, 2015, **7**, 3817-3837.
- 41 J. Sekine, S. C. Luo, S. Wang, B. Zhu, H. R. Tseng and H. H. Yu, *Adv. Mater.*, 2011, **23**, 4788-4792.